Molecular Beam Study on Oxidation of Si(100) Surface with Ozone

I. Kinefuchi[1], H. Yamaguchi[2], Y. Sakiyama[1], and Y. Matsumoto[1]

[1] *Department of Mechanical Engineering, The University of Tokyo, 7-3-1 Hongo Bunkyo-ku, Tokyo 113-8656, Japan*
[2] *Graduate School of Micro-Nano system engineering, Nagoya University, Furo-cho, Chikusa-ku, Nagoya, Aichi 464-8603, Japan*

Abstract. The reaction of O_3 with Si(100) surface has been investigated by employing supersonic molecular beam techniques. The temperature programmed desorption (TPD) analysis of the oxide adlayers formed by an O_3 molecular beam showed that O_3 enhances the oxidation rate especially on low coverage surfaces and forms stable oxide adlayers as compared with O_2. These results are attributed to O atoms generated from the decomposition of O_3 on the surface at elevated temperature. The reaction path involving these O atoms was confirmed by the larger rate constants of the intermediate oxide formation than those with O_2 molecules in the modulated molecular beam reactive scattering (MMBRS) experiments.

Keywords: Gas-surface interaction; Molecular beam; Temperature programmed desorption; Reactive scattering; Silicon; Ozone; Oxidation
PACS: 34.50.Lf, 68.47.Fg, 82.65.+r

INTRODUCTION

The low temperature oxidation of silicon surface is a key issue for the fabrication process of polysilicon thin film transistors (poly-Si TFTs) on non-heat-resistant substrates such as glass and plastics, since these substrates restrict the process temperature to far less than that of the conventional thermal oxidation in pure O_2 ambient. Although plasma enhanced chemical vapor deposition (PECVD) is the most common method at present for the temperature less than 600 °C, the degradation of the film quality caused by the energetic ions colliding with the substrates prevents the further downscaling of the devices. The oxidation of silicon surface with ozone (O_3) has recently received much attention for potential application to this process since O_3 enhances the growth rate of SiO_2 films significantly without the production of any deteriorating ions.

Several groups [1-3] have investigated the oxidation rates of Si(100) surface in the atmosphere of O_3 / O_2 gas mixture for a wide range of O_3 concentration, the ambient pressure, and the surface temperature. In the most effective cases, they found that the growth rates induced under these conditions are more than one order of magnitude larger than those achieved using the conventional thermal oxidation in pure O_2 atmosphere. Unfortunately, the enhancement effect of O_3 on the oxidation rates reported to date strongly depends on the specific geometry of each reaction chamber because of the thermal decomposition of O_3 to O_2 in the gas phase, which leads to the ambiguous concentration of O_3 in the incident gas flux to the substrates and obscures the detailed understanding of the elementary reaction steps on the surface.

The aim of our study is to elucidate the initial oxidation stage of Si(100) surface with O_3, especially in the low coverage regime. We have employed the supersonic molecular beam technique to investigate this reaction because it enables us to exclude the gas phase reaction and thus to conduct the experiment in a well-controlled fashion. In this paper, we examined the oxide adlayers formed by the beam exposure with temperature programmed desorption (TPD) [4] and discussed the oxidation kinetics and the structure of these adlayers. In addition, the reaction dynamics of O_3 and clean Si(100) surface was also analyzed in detail by use of modulated molecular beam reactive scattering (MMBRS) [5], in which the reaction product desorbing from the surface was detected with a time resolution of several microseconds.

TABLE 1. Characteristics of molecular beams used in our work.

Beam	Translational Energy [eV]	Intensity [molecules/cm^2·s] O_3	Intensity [molecules/cm^2·s] O_2
O_2 (pure)	0.08	-	1×10^{15}
Low-concentrated O_3 (5.1% O_3 / O_2)	0.13 (for O_3)	6×10^{13}	1×10^{15}
High-concentrated O_3 (~60% O_3 / O_2, diluted with He)	0.18 (for O_3)	9×10^{13}	7×10^{13}

EXPERIMENTAL SETUP

The experiments were conducted in an ultrahigh vacuum chamber equipped with a supersonic molecular beam source. The configuration of our setup was roughly the same as described previously [6] although it was slightly modified for this work. The vacuum chamber was evacuated with a series connection of two turbomolecular pumps and a liquid nitrogen cold trap. The base pressure was ~1×10^{-7} Pa. During the irradiation of the molecular beam, the large pumping speed always maintained the pressure in the 10^{-7} Pa range.

The molecular beam source consisted of three differential pumping stages, which collimated the beam so that the spot diameter at the sample surface was about 5 mm. The beam was square-wave modulated, if necessary, by a rotating chopper with a duty cycle of 25%. The characteristics of three types of molecular beams we used in this work are summarized in Table 1. In order to prepare the oxide adlayers for TPD experiments, we employed the low-concentrated O_3 gas (5.1% O_3 / O_2), which was generated by a barrier discharge ozonizer and the concentration of which was monitored with a polarographic membrane-type sensor. The high-concentrated O_3 gas (~60% O_3 / O_2) diluted with He, commercially available from Iwatani Gas corp., was applied for the reactive scattering experiments. In the both experiments, pure O_2 beam was used for comparison against O_3.

A quadrupole mass spectrometer was mounted on a positioning assembly which consisted of a linear stage and a differentially-pumped rotary platform. The mass spectrometer could be rotated around the sample manipulator with keeping the distance between the sample surface and the ionizing region of the mass spectrometer in the range of 49 to 186 mm. In this work, the mass spectrometer was placed as close as possible to the sample surface in order to maximize the sensitivity to the reaction product.

We used square-shaped substrates with the size of 10 × 10 × 0.525 mm, which were diced from polished p-type Si(100) wafers with resistivity of 9 - 12 Ωcm. The samples were cleaned using the standard RCA procedure [7] followed by a dip in dilute HF (~1%) to remove the oxide on the surface. They were loaded to the sample manipulator in the vacuum chamber through a load lock system without breaking vacuum and were annealed at ~400 °C for outgassing. Before each experiment, the sample was heated to 1000 °C in vacuum to remove the residual oxide layer and was cooled down to a target temperature with a rate of 1 - 2 K/s to obtain the surface having a low defect density. The temperature of the surface was checked with infrared thermometers operating at the wavelength around 1 μm. During the series of experiment, the incident beam angle and the detector angle were fixed at 40° and 20°, respectively, from the surface normal.

RESULTS AND DISCUSSION

Temperature Programmed Desorption

To clarify the mechanism of the initial oxidation process of Si(100) surface with O_3, we analyzed the oxide adlayers grown by O_3 using TPD technique. Oxide adlayers were formed on clean Si(100) surfaces by the exposure of pure O_2 beam and 5.1%-O_3 / O_2 beam. We kept the temperature of the substrates at 673 K during the beam exposure. Subsequently, the desorption spectra of SiO molecules (m/e = 44), which were produced from the decomposition of the oxide adlayers, were taken with a liner heating rate of 4 K/s. The quadrupole mass spectrometer, with which the desorption rates were measured, was calibrated by means of the saturation coverage of H_2O on the Si(100) surface since a saturated exposure of H_2O on Si(100) surface at room temperature produces 0.5 ML each of OH(a) and H(a) [8].

Figure 1 shows the desorption spectra from the oxide adlayers, the oxygen coverages of which are less than 3 monolayers (1 ML = 6.8×10^{14} atoms/cm^2). The desorption spectrum exhibits a single large peak for all the samples although an additional small peak emarges as the oxygen coverage increases. These multimodal spectra indicate the heterogeneity of the structure induced by the strong mutual interaction between adatoms with high areal density.

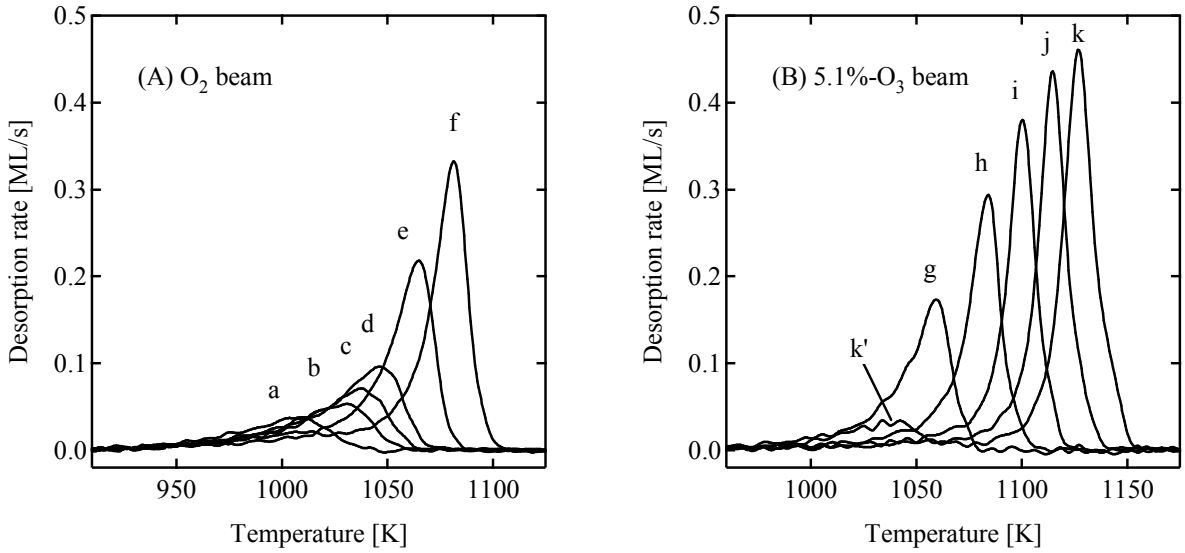

FIGURE 1. Thermal desorption spectra of SiO from oxide adlayers. (A) The oxide adlayers formed by pure O_2 beam. The initial coverages from a to f are 0.53, 0.74, 0.89, 1.13, 1.74 and 2.28 ML. (B) The oxide adlayers formed by 5.1%-O_3 beam. The initial coverages from g to k are 1.4, 1.8, 2.0, 2.3 and 2.8 ML.

Regardless of which molecular beam was applied, as the oxygen coverage increases, the adlayer has more stable structure, which can be confirmed from the shift of the main peaks (i.e. the largest peaks) to higher temperature. Moreover, the films grown with 5.1%-O_3 / O_2 beam exhibit higher peak temperatures than those of the same coverage grown with pure O_2 beam. Thus the incidence of O_3 on the surface results in the more stable geometry of the oxygen adatoms than that of O_2. This is attributed to O atoms, which is much more reactive than O_2, generated by the decomposition of the incident O_3 molecules on the surface.

The decomposition of the oxide adlayer does not follow a first-order kinetics, which assumes homogeneous reaction where each SiO molecule desorbs independently. Several STM observations [9-11] have reported that oxide adlayer on silicon surface decomposes inhomogeneously with void formation, which suggests that each adatom suppresses the desorption rate of adjacent adatoms. Therefore, we have to take account of surface morphology during the decomposition to obtain the desorption rate equation. A detailed discussion will be given elsewhere.

Figure 2 shows the oxygen coverage determined from the integrated area of each desorption spectrum as a function of beam exposure time. The dependence of the adsorption probability S, which is propotional to the gradient of the oxygen uptake curves $d\theta(t)/dt$, on the coverage follows modified Langmuirian kinetics:

$$S(\theta) = S_0\left(1-\theta/\theta_{\mathrm{sat}}\right)^d, \tag{1}$$

where θ is the oxygen coverage, θ_{sat} the saturation coverage, S_0 the initial sticking probability and d the order of the reaction. d is interpreted as a measure of a strength of the interaction between adatoms which reduce the sticking probability of the adjacent reaction sites. The oxygen coverage is given by

$$\theta(t) = \int_0^t F S(\theta)\, dt, \tag{2}$$

where F is an incident flux of molecules on the surface. From numerical fittings of Eq. (2) to the experimental results, we determined the saturation coverages for pure O_2 beam and 5.1%-O_3 / O_2 beam to be 2.70±0.13 ML and 4.96±1.35 ML respectively. These saturation coverages correspond to areal density of reaction sites. During exposure of pure O_2 beam, O atoms are inserted only into dimer bridge and dimer backbond sites. Since the total areal density of these sites is 2.5 ML, few O atoms prove to be capable of occupying subsurface backbonds. This result is consistent with DFT calculations by Kato et al. [12]. They have reported that there are barrierless oxidation paths for dimer bridge sites and dimer backbond sites whereas the activation energy for oxidation of subsurface backbounds is at least 2.4 eV, depending on the incident position and the orientation of an O_2 molecule. The relatively high activation energy reduces the oxidation rate of subsurface backbonds significangly because of the low surface temperature ($k_B T_s$ ~ 0.06 eV) and low incident energy of gas molecules (~0.1 eV) during the oxidation. In

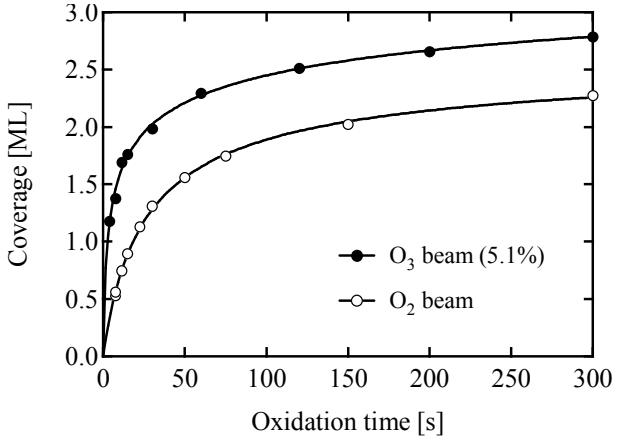

FIGURE 2. Oxygen coverage as a function of beam exposure time. Solid lines are fitting curves determined from numerical fittings of modified Langmuirian kinetics (Eq. (1) and (2)).

contrast, exposure of 5.1%-O_3 / O_2 beam leads to saturated adlayer with O atoms sitting at not only dimer bridge and backbond sites but also subsurface backbonds. The total areal density of these sites is 4.5 ML, which is fairly close to the saturation coverage obtained from our experiment. There should be very small activation barrier, if any, for the oxidation of subsurface backbonds with O_3. The high reactivity of O_3 is due to O atoms produced from the decomposition of O_3 on Si surface at elevated temperature. The reactive scattering experiment described in the next section also supported that the reaction path involving O atoms enhances the reaction rate of the adsorption process.

Molecular Beam Reactive Scattering

We also conducted molecular beam reactive scattering experiments to investigate the reaction dynamics on the surface. The samples at temperatures more than 1053 K were exposed to the high concentrated O_3 beam (see Table 1), and also pure O_2 beam for comparison. The oxidation process of Si surface depends on the surface temperature and the incident flux of oxidant molecules onto the surface. At low substrate temperature and high incident flux, the reaction leads to the formation of stable oxide SiO_2(s). On the other hand, at high temperature and low incident flux, the surface is etched with the desorption of volatile product 2SiO(g). These processes are called "passive" and "active" oxidation, respectively. D'Evelyn et al. [13] and Yu et al. [14] reported that the active oxidation with pure O_2 beam follows the two-step first-order reaction process:

$$\mathrm{Si(s)} + 1/2\,\mathrm{O_2} \xrightarrow{s} I_1 \xrightarrow{k_1} I_2 \xrightarrow{k_2} \mathrm{SiO(a)}\uparrow . \tag{3}$$

In this process, O_2 adsorbs dissociatively on the surface with a sticking probability s and forms a nonvolatile intermediate oxide I_1 on the surface. This intermediate oxide I_1 is then converted into a desorption precursor I_2 at a rate k_1. Finally SiO desorbs from the surface at a rate k_2. Exposing the sample surface to the square-wave modulated molecular beam, we measured the desorption flux of product molecules SiO from the surface as a function of time using a quadrupole mass spectrometer. Since the intermidiate oxide on the surface desorbs with short residence time (~100μs), the oxygen coverage remains substantially zero, insofar as the incident beam flux is small enough. Thus, we can observe the reaction dynamics on "clean" surface without any interference between adatoms.

Figure 3 shows waveforms of SiO mass spectrometric intensity at various substrate temperatures. The beam modulation is also shown as a solid line for reference. This result shows the strong dependence of the reaction rate on temperature. The signal of the reaction product $Q(t)$ can be described by a convolution of the incident flux of the molecular beam onto the surface $R(t)$, the surface residence time (i.e. the time required for completion of the reaction) $T(t)$ and the time-of-flight (TOF) distribution of the product molecules from the surface to the detector $P(t)$:

$$Q(t) = [R * T] * P(t) = \int_0^t \left[\int_0^{t-\tau} R(t-\tau-z)\, T(z)\, dz \right] P(\tau)\, d\tau , \tag{4}$$

where $R(t)$ is already known from the TOF measurement of the incident beam before the scattering experiments. In

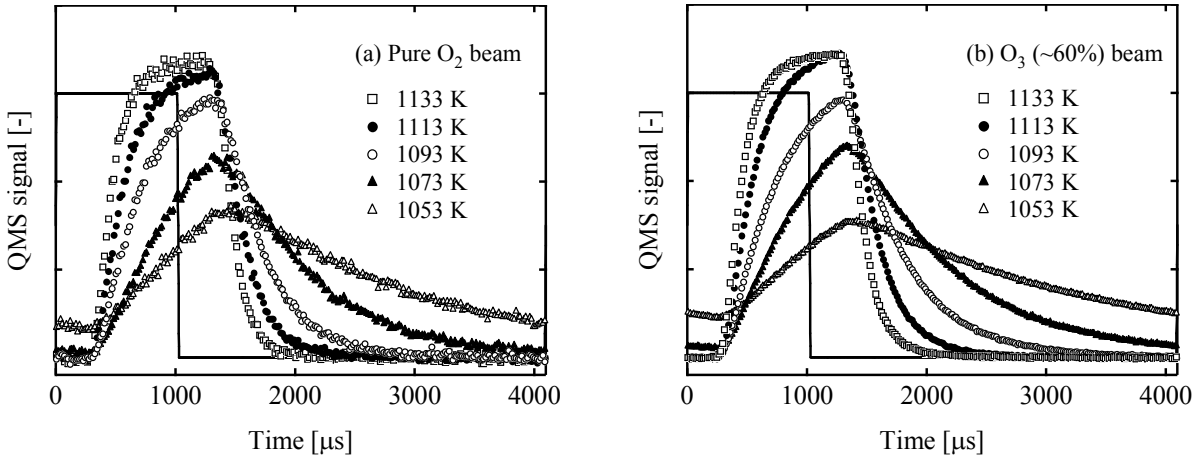

FIGURE 3. Waveforms of the reaction product SiO desorbing from the surface.

addition, $P(t)$ follows Maxwell-Boltzmann distribution at the surface temperature since we can reasonably assume full accommodation of product molecules desorbing from the surface. Therefore, the surface residence time $T(t)$ can be determined from the experimental waveform $Q(t)$, in principle, by deconvoluting Eq.(4), although noise component in the waveform makes it practically difficult to perform direct numerical deconvolution.

The surface transfer function $\widetilde{T}(\omega)$, i.e. Fourier transform of the surface residence time distribution, gives us quantitative as well as qualitative information on the reaction mechanism. From Eq.(4) we obtain

$$\widetilde{T}(\omega) = \widetilde{Q}(\omega) \,/\, [\widetilde{R}(\omega)\,\widetilde{P}(\omega)] \,. \tag{5}$$

In Fig. 4 surface transfer functions are plotted in the complex plane for qualitative interpretation. The phase lag of the transfer function with ~60% O_3 beam at high frequency is less than that with pure O_2 beam. As in the case with pure O_2 beam, the reaction with O_3 is also well reproduced by the sequential two-step first-order reaction model:

$$\mathrm{Si(s)} + 1/3\,\mathrm{O_3} \xrightarrow{s'} I_1' \xrightarrow{k_1'} I_2' \xrightarrow{k_2'} \mathrm{SiO(a)}\uparrow . \tag{6}$$

The reaction rates k_1', k_2' were determined with a numerical fitting method assuming the theoretical response function, which is derived from the mass balance equations of this model. As shown in Fig. 5, the temperature dependence of these rates follows Arrhenius equation except at 1053 K, where transition of active to passive oxidation occurs. When the surface is exposed to ~60% O_3 beam, the reaction rate of the first step k_1' is at least two times larger than that with pure O_2 beam k_1. This result suggests that there is another reaction path for the desorption precursor generation involving atomic oxygen due to the decomposition of O_3 on the surface. On the other hand, the reaction rate of the second step k_2' above the transition temperature is almost the same as that with pure O_2 beam k_2. This means that the desorption precursor (I_2 and I_2') has the identical structure for both cases.

CONCLUSION

The reaction of O_3 with Si(100) surface was investigated by employing molecular beam techniques. The TPD analysis showed that O_3 enhances the oxidation rate especially on low coverage surfaces and forms stable oxide adlayers as compared with O_2. These results are attributed to O atoms generated from the decomposition of O_3 on the surface at elevated temperature. The reaction path involving these O atoms was confirmed by the larger rate constants of the intermediate oxide formation than those with O_2 molecules in the reactive scattering experiment.

ACKNOWLEDGMENTS

The present work was supported in part through the 21st Century COE Program, “Mechanical Systems Innovation,” by the Ministry of Education, Culture, Sports, Science and Technology.

REFERENCES

1. T. Nishiguchi, H. Nonaka, S. Ichimura, Y. Morikawa, M. Kekura, and M. Miyamoto, *Appl. Phys. Lett.* **81**, 2190-2192 (2002).
2. Z. Cui et al., *J. Electrochem. Soc.* **150**, G694-G701 (2003); *J. Appl. Phys.* **87**, 8181-8186 (2000).
3. A. Kazor et al., *Appl. Phys. Lett.* **65**, 412-414 (1994); *Appl. Phys. Lett.* **63**, 2517-2519 (1993).
4. P. A. Redhead, *Vacuum* **12**, 203-211 (1962).
5. M. L. Yu and L. A. DeLouise, *Surf. Sci. Rep.* **19**, 285-380 (1994).
6. I. Kinefuchi, H. Yamaguchi, Y. Sakiyama, and Y. Matsumoto, *Proc. 24th Int. Symp. on R.G.D.*, 947-952 (2005).
7. W. Kern, *J. Electrochem. Soc.* **137**, 1887-1892 (1990).
8. D. Schmeisser, *Surf. Sci.* **137**, 197-210 (1984); W. Ranke and Y. R. *Xing, Surf. Sci.* **157**, 339-352 (1985).
9. K. E. Johnson and T. Engel, *Phys. Rev. Lett.* **69**, 339-342 (1992).
10. Y. Wei, R. M. Wallace, and A. C. Seabaugh, *Appl. Phys. Lett.* **69**, 1270-1272 (1996).
11. Y. Kobayashi, *J. Vac. Sci. Technol. B* **9**, 748-751 (1991).
12. K. Kato et al., *Phys. Rev. Lett.* **80**, 2000-2003 (1998); *Phys. Rev. B* **62**, 15978-15988 (2000).
13. M. P. D'Evelyn, M. M. Nelson, and T. Engel, *Surf. Sci.* **186**, 75-114 (1987).
14. M. L. Yu and B. N. Eldridge, *Phys. Rev. Lett.* **58**, 1691-1694 (1987).

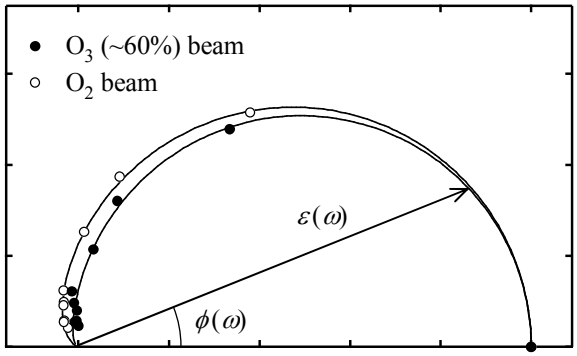

FIGURE 4. Surface transfer functions (Eq.(5)) derived from the experimental waveforms of the product molecules SiO. The theoretical transfer functions of the two-step first-order reaction model are also plotted as solid lines.

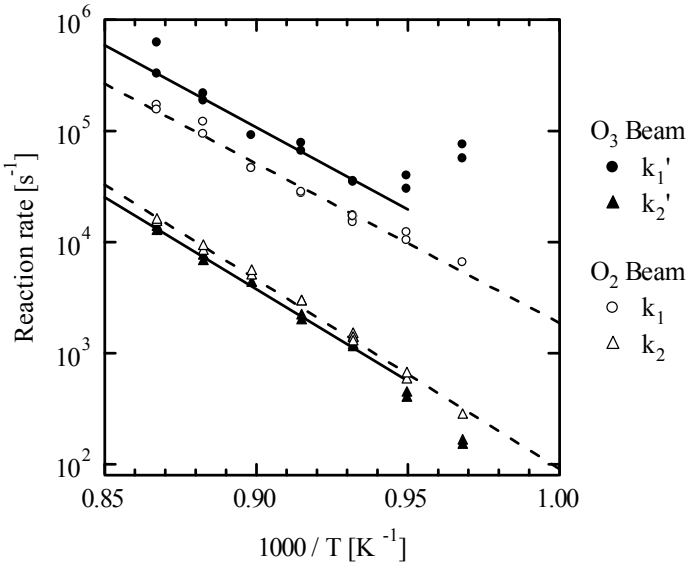

FIGURE 5. Reaction rate constants of the elementary steps in Eq.(3) and Eq.(6). Solid and dashed lines represent Arrhenius equations fitted to the experimental results.